Glycation alters the mechanical behavior of kidney extracellular matrix

Snehal Sant[a], **Dan Wang**[a], **Rishabh Agarwal**[a], **Sarah Dillender**[a] and **Nicholas Ferrell**[a, b, c]

a - *Department of Medicine,* Division of Nephrology, Vanderbilt University Medical Center, United States of America
b - *Department of Biomedical Engineering,* Vanderbilt University, United States of America
c - *Vanderbilt Center for Kidney Disease,* United States of America

*Correspondence to Nicholas Ferrell:*at: 1161 21st Ave. South, S3223 Medical Center North, Nashville, TN 37212, United States of America. nick.ferrell@vanderbilt.edu
https://doi.org/10.1016/j.mbplus.2020.100035

Abstract

The mechanical properties of the extracellular matrix (ECM) are important in maintaining normal physiological function, and changes in ECM mechanics drive disease. The biochemical structure of the ECM is modified with aging and in diseases such as diabetes. One mechanism of ECM modification is the non-enzymatic reaction between sugars and ECM proteins resulting in formation of advanced glycation end products (AGEs). Some AGE reactions result in formation of molecular crosslinks within or between matrix proteins, but it is not clear how sugar-mediated biochemical modification of the ECM translates to changes in kidney ECM mechanical properties. AGE-mediated changes in ECM mechanics may have pathological consequences in diabetic kidney disease. To determine how sugars alter the mechanical properties of the kidney ECM, we employ custom methodologies to evaluate the mechanical properties of isolated tubular basement membrane (TBM) and glomerular ECM. Results show that the mechanical properties of TBM and glomerular ECM stiffness were altered by incubation in glucose and ribose. Mechanical behavior of TBM and glomerular ECM were further evaluated using mechanical models for hyperelastic materials in tension and compression. Increased ECM stiffness following sugar modification corresponded to increased crosslinking as determined by ECM fluorescence and reduced pepsin extractability of sugar modified ECM. These results show that sugar-induced modifications significantly affect the mechanical properties of kidney ECM. AGE-mediated changes in ECM mechanics may be important in progression of chronic diseases including diabetic kidney disease.

Introduction

The extracellular matrix (ECM) is a complex three-dimensional assembly of proteins that provides support for cells throughout the body. In addition to acting as a structural framework, the ECM also provides biochemical and biophysical cues to adherent cells that are critical drivers of cell function [1,2]. The mechanical properties of the ECM are important in regulating cell proliferation, differentiation, migration and cell survival [3–5]. Disease-mediated stiffening of the ECM alters cellular function and contributes to progression of cancer, cardiovascular disease, and fibrosis [6–11]. While increased ECM stiffness in cancer and fibrosis has largely been attributed to upregulation of enzymatic crosslinking [12,13], additional non-enzymatic mechanisms of ECM stiffening may be relevant to pathological conditions such as diabetes.

Diabetes is the most common cause of end-stage renal disease. While a number of complex factors contribute to kidney damage in diabetes, one factor that plays a role in disease progression is formation of advance glycation end-products (AGEs) [14].

AGEs are a heterogeneous group of biochemical modifications that form through the non-enzymatic reaction between sugars or other reactive carbonyls with amine groups on proteins. This process is accelerated in diabetes and leads to accumulation of AGEs in the kidney ECM [15,16]. Some AGEs bridge multiple amino acids to form crosslinks that have been shown to alter the mechanical properties of load bearing tissues rich in fibrillar collagens such as bone, tendon, and cartilage [17–19]. It is not clear how sugar-induced biochemical modifications translate into altered mechanical properties of the glomerular matrix and tubular basement membrane (TBM), which are composed primarily of networked collagen IV and laminin along with nidogens, heparin sulfate proteoglycans, and other structural and regulatory proteins [20–22].

In this study, we introduce a novel method of characterizing the mechanical properties of the glomerular matrix using a microcantilever based compression assay. This technique is a variation of a previously developed method for analyzing basement membrane stiffness in tension [23,24]. Using these two methods, we evaluated the effects of glucose and ribose modification on the mechanical properties of the ECM from the two primary functional components of the kidney, the glomerulus and the tubule. Mathematical modeling was used to evaluate the force-displacement response of TBM and glomerular ECM. AGE formation by glucose or ribose altered the mechanical behavior of TBM and glomerular ECM. This demonstrates that glycation directly modifies the mechanical properties of the kidney ECM. Increases in stiffness were accompanied by increased matrix crosslinking as determined by ECM fluorescence and reduced pepsin extractability of glycated matrix. These studies introduce a novel method to analyze the mechanical behavior of glomerular ECM, provide a mathematical framework to evaluate the non-linear mechanical behavior of the ECM, and show that sugar-mediated crosslinking significantly alters the mechanical behavior of the kidney ECM.

Results and discussion

In this study, we introduce a new method to evaluate the compressive stiffness of decellularized glomerular extracellular matrix. This is a modified version of our previously described approach for characterizing the mechanical properties of basement membranes in tension [23,24]. Collectively, these custom measurement techniques allowed for characterization of the mechanical behavior of the ECM from renal glomeruli and tubules, the two primary functional components of the kidney.

Tubular basement membrane exhibited significant non-linearity in the stress-strain response as is evident from the experimental data in Fig. 1. This strain stiffening response, or increase in stiffness with increased strain, is typical of many biological materials, including crosslinked actin networks, collagen gels, and blood vessels [25–28]. Strain-stiffening behavior is highly influenced by network mechanics, that is the complex three-dimensional interactions between different components in the network rather than purely the mechanical properties of the individual components themselves. This non-linear response was blunted by sugar modification, particularly by ribose. The physiological importance of this non-linear response or the reduction in this effect following glycation is not yet clear in this context. However, several studies show that non-linear mechanics of the ECM has functional consequences for cellular behavior. Strain-stiffening as well as stress relaxation have been shown to affect cell migration [29], stem cell differentiation [30], cell spreading [31], and the transmission of mechanical signals between cells [32]. Most in vitro studies on the effects of altered mechanical properties on cell behavior rely on elastic hydrogels that do not recapitulate the complex non-linear behavior of in vivo matrices. More sophisticated in vitro models that better recapitulate the complex mechanical behavior of the ECM have recently been developed [33,34], and may give important new insight into the role of ECM mechanics in regulated cell function under more physiologically relevant conditions and may be useful for gaining additional insight into how changes in mechanical behavior contribute to disease progression.

The stress-strain response of the TBM was evaluated using the Humphrey's model of hyperelastic materials. This model was originally developed to describe the passive mechanical response of myocardial tissue and has been shown effective
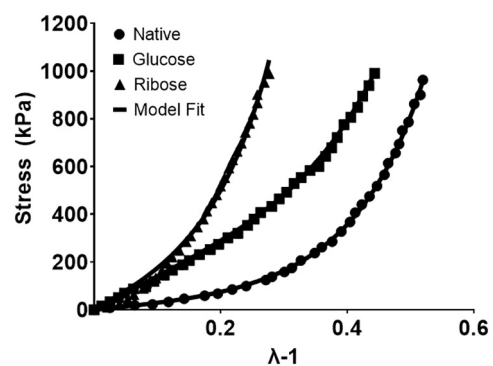
Fig. 1. Stress-strain response for native and sugar modified tubular basement membrane. Unmodified basement membrane (●) exhibits significant non-linearity. Glucose (■) and ribose (▲) modified basement membranes show an upward shift in the stress-strain response indicating increased resistance to deformation. Data are fit to the Humphrey's model of hyperelasticity. Model fits are in good agreement with experimental data.

for modeling soft tissue mechanics [35–37]. Experimental data were in good agreement with the model fits under uniaxial tension for both native and sugar-modified basement membranes (Fig. 1). Glucose and ribose both modified the stress-strain response of the TBM. Ribose had the most significant impact on the mechanical response. This is expected based on the much higher reactivity of ribose with amino acids as compared to glucose [38]. Ribose has commonly been used to study AGE formation in vitro in more pragmatic time scales [39,40]. However, it should be noted there are not only differences in reactivity between glucose and ribose, but these sugars result in the formation of biochemically distinct crosslinks. In vitro, ribose leads to formation of significantly higher amounts of pentosidine crosslinks compared to glucose [41]. However, glucosepane is the primary crosslink found in the extracellular matrix in vivo [15]. The mechanical behavior of unmodified TBM was similar to what we observed previously [23]. Small differences in the stress-strain response likely result from a loss of mechanical stiffness during the incubation period, differences in baseline mechanical properties between different mouse strains, or differences in the basement membrane thickness.

The material fitting parameters c_1 and c_2 for native and sugar modified tubular basement membranes are shown in Table 1. This showed that for ribose modification c_2 was significantly increased. Given the dramatic difference in the stress-strain response in ribose modified tubules, it is consistent with this modifying the exponential term in the model. It is difficult to ascribe physical meaning to variations in the fit parameters. To provide a more intuitive comparison of the mechanical properties between conditions, the tangent modulus was calculated by taking the derivate of the model fit equations. The tangent modulus was taken at 20% and 30% strain for ribose and glucose modified tubules. Tangent modulus of ribose modified TBM was approximately 5 times higher in ribose modified TBM at 20% strain. Tangent modulus for glucose modified TBM was elevated at 20% and approached statistical significance (adjusted $p = 0.07$) and reached statistical significance at 30% strain. Given the relatively high

resistance of ribose modified TBM to tensile deformation, it was rare for these tubules to achieve 30% strain, so no data is reported for tangent modulus of ribose modified TBM at higher strain.

Unlike tubular tensile behavior, the cellular contribution to glomerular resistance in compression plays an important role in mechanical response. We found that the measured stiffness was significantly reduced following decellularization (data not shown). This is similar to what has been observed using other techniques to evaluate glomerular stiffness [42]. The difference in cellular contributions to the mechanical response in glomeruli versus tubules is likely due primarily to tension/compression asymmetry in the extracellular matrix. Many biological materials behave differently under tensile versus compressive loading with regard to their mechanical response. TBM demonstrates significant resistance to tensile deformation as demonstrated by the high tangent modulus. TBM tangent modulus was on the order of 1 MPa, even at lower strain. By contrast, tensile stiffness of cell monolayers is approximately 20 kPa [43]. As such, the TBM stiffness dominates the mechanical response. For glomeruli in compression, the stiffness of the glomerular ECM is on the same order of magnitude as that of cells in compression which have been measured by atomic force microscopy to be 300–400 Pa for cultured epithelial cells in compression [44]. Therefore, the cellular component of the response is significant. Given our specific interest in ECM properties, glomeruli were decellularized prior to analysis. However, the methodology as well as the mathematical models used to describe the force-displacement response are applicable to cellularized or decellularized glomeruli from multiple species. Additionally, this methodology may be applied to other soft spherical microstructures and could be applicable to a number of additional applications.
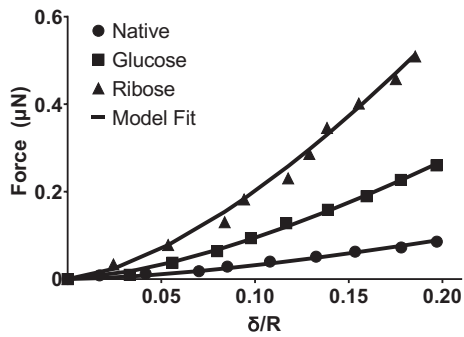
Glomerular force-displacement response was modeled using an expanded Hertz model described by Tatara for compression of a sphere between two flat plates. Similar to the TBM, the model was in reasonable agreement with the experimental data (Fig. 2) and allowed for evaluation of the low strain (<20%) elastic modulus (E). The glycated glomerular

Table 1. Comparison of model fit parameters and tangent modulus for native and glycated tubular basement membrane.

| Modification	c_1	c_2	Tangent modulus (kPa) (20% strain)	Tangent modulus (kPa) (30% strain)
Native ($n = 10$)	52.5 ± 12.5	2.10 ± 0.31	939 ± 102	1671 ± 233
Glucose ($n = 8$)	116.3 ± 28.0	1.94 ± 0.29	1828 ± 177	3063 ± 360[*]
Ribose ($n = 9$)	52.3 ± 5.7	4.86 ± 0.40[*,**]	5380 ± 854[*]	NA

[*] Denotes statistically significant difference (p<0.05) as compared to native tubular basement membrane.
[**] Denotes statistically significant difference (p<0.05) between glucose and ribose. Data were analyzed by Kruskal-Wallis H testing follow by post-hoc Mann-Whitney U testing. Data are shown as mean ± standard error of the mean (SEM).

Fig. 2. Force-displacement response of native and sugar modified glomerular ECM. Sugar modification resulted in an upward shift in the force-displacement response indicating increased resistance to compression. Data were fit to the modified Hertz model described by Tatara for glomerular compression up to 20%. Models fits were in good agreement with the experimental data.

matrix showed an increase in stiffness following glucose modification but did not reach statistical significance. Ribose modification resulted in a significant increase in mean glomerular matrix stiffness (Fig. 3). This is consistent with the behavior seen in ribose modified TBM, with ribose showing a more pronounced impact on ECM stiffness compared to glucose. This also shows that if sufficient crosslinking is induced, the compressive properties of the glomerular ECM are modified. The more significant increase in glomerular compressive stiffness following ribose modification as compared to
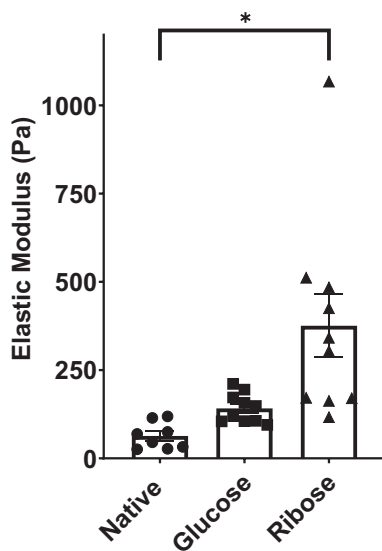
Fig. 3. Elastic modulus of decellularized native ($n = 8$), glucose ($n = 10$), and ribose modified ($n = 10$) glomerular ECM as determined from the best fit of the Tatara model. Data is shown at the mean ± SEM. * denotes statistical significance ($p < 0.05$) based on Kruskal-Wallis H testing follow by post-hoc Mann-Whitney U testing.

glucose is likely due to multiple factors. First, time scales needed for glucose-mediated reactions to run to completion are significantly longer than for ribose [45]. Additionally, the model employed for analyzing glomerular matrix stiffness is only valid up to 20% glomerular compression. Similar to the behavior of TBM, it is likely that the effects of crosslinking on the mechanical response are more pronounced at higher strains. Finally, crosslinking of the ECM may have more impact on the tensile properties as compared to compressive properties based on crosslinks limiting the ability of the matrix to expand in tension compared to the buckling response in compression.

Immunofluorescence imaging for structural ECM proteins (collagen IV and laminin) in the decellularized glomeruli show that both were retained in the matrix following detergent extraction of cells (Fig. 4a) and the three-dimensional architecture of the matrix was largely retained with defined glomerular capillary loops evident as indicated with arrows in Fig. 4a. Exposure matched (no primary antibody) negative controls for collagen IV and laminin are shown in the supplementary data (Supplementary Fig. 1). Counterstaining with DAPI (Fig. 4b) showed minimal residual nuclear material following decellularization. Western blotting further confirmed retention of laminin and collagen IV in the decellularized glomeruli (Fig. 4c).

To evaluate formation of advanced glycation end products in sugar-modified ECM, total fluorescence was measured in acid hydrolyzed and reconstituted ECM. Fluorescence intensity increased following glucose and ribose incubation (Fig. 5) with glucose showing a modest increase in intensity while ribose showed a significant increase in fluorescence intensity. This likely reflects both the increased reactivity of ribose and the propensity for ribose to form fluorescent AGEs such as pentosidine as opposed to non-fluorescent glucose derived crosslinks. To further evaluate crosslinking, relative pepsin extractability was measured and the ratio of collagen content in the pepsin soluble and insoluble fractions were used as a measure of crosslinking. Both glucose and ribose modified ECM showed dramatic reductions in pepsin extractability with reductions of approximately 80% in glucose modified ECM and 90% in ribose modified matrix.

AGEs have been recognized as pathological contributors to progression of diabetic nephropathy through multiple mechanisms. Receptor-mediated effects include binding the cellular receptor for AGEs (RAGE) to elicit pro-inflammatory and pro-fibrotic cellular pathways that contribute to disease pathology [46,47]. Non-receptor mediated effects include reduction in extracellular matrix susceptibility to proteolytic degradation that reduces ECM turnover and may contribute to ECM accumulation [48]. AGE-mediated crosslinking and stiffening of the ECM may
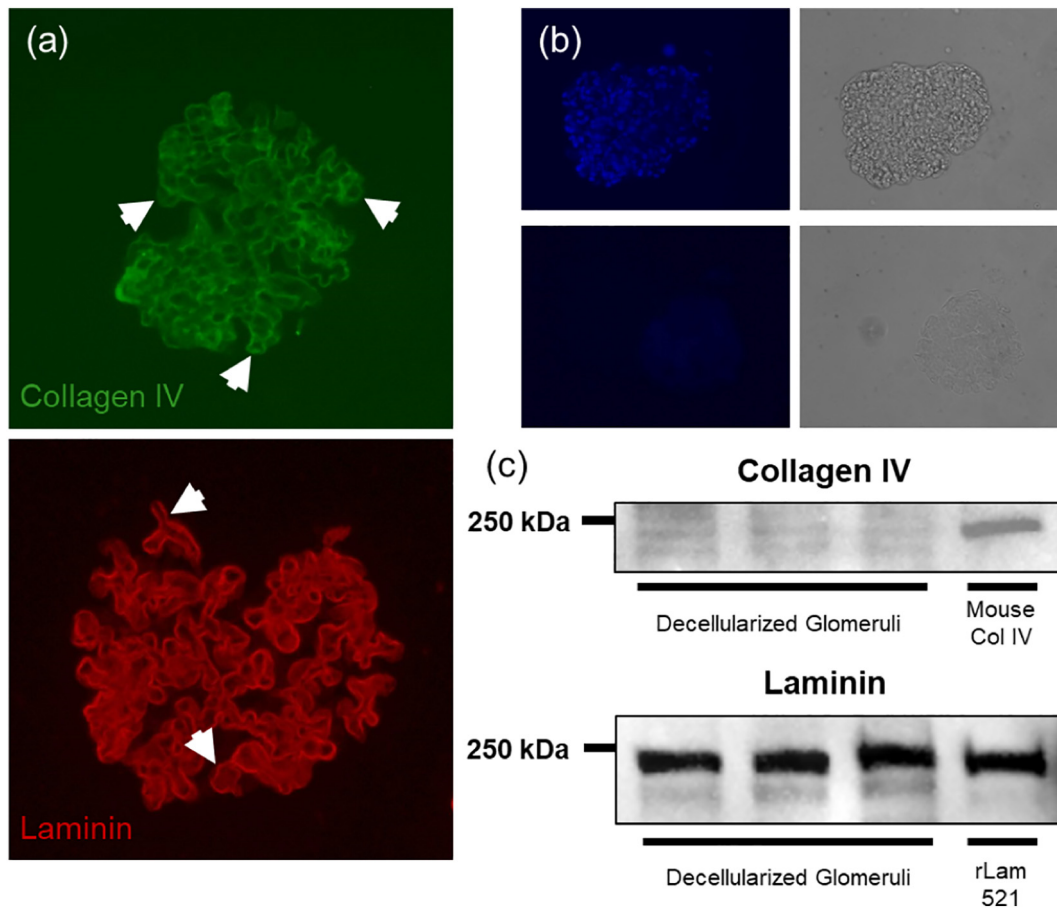
Fig. 4. (a) Collagen IV and laminin immunostaining in decellularized glomeruli showing retention of structural matrix proteins following decellularization. (b) DAPI staining before and after decellularized shows that minimal residual DNA was present in the glomerular matrix following decellularization. (c) Western blotting of decellularized glomerular ECM further confirmed retention of ECM structural proteins. Mouse collagen IV and recombinant human Laminin 521 were used as positive controls.

be an additional mechanism that contributes to cellular dysfunction in diabetes.

Conclusions

The mechanical properties of the extracellular matrix are important for both maintaining normal physiological function and for mediating disease progression. In this study, we show that sugar modifications have a significant effect on the mechanical behavior of kidney extracellular matrix. We introduce a new technique to characterize the mechanical behavior of glomerular ECM in compression. This technique is generally applicable for characterizing the mechanical properties of spherical microstructures in compression. Given the significance of enzymatic crosslinking and stiffening of the ECM to tissue dysfunction in cancer, fibrosis, cardiovascular disease, and aging, non-enzymatic mechanisms of ECM stiffening may similarly have

pathological importance in diabetes both in the kidney and in other organs and tissues. This study shows that sugar induced biochemical modifications directly modify the mechanical behavior of both glomerular and tubular ECM and motivate further investigation into how these biomechanical changes contribute to pathological cellular responses in diabetic kidney disease.

Materials and methods

Isolation of tubules and glomeruli

Animals were treated in accordance with the National Institutes of Health (NIH) Guide for the Care and Use of Laboratory Animals, and all procedures were approved by the Institutional Animal Care and Use Committee of Vanderbilt University Medical Center. Renal tubules were
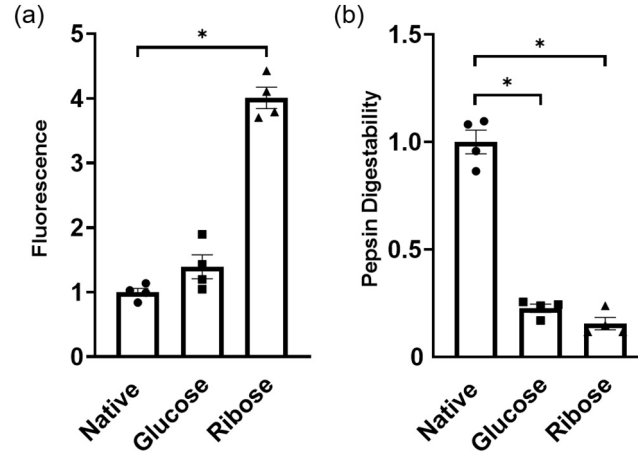
Fig. 5. (a) Fluorescence intensity (ex./em. 365/415–445 nm) for native and sugar modified ECM ($n = 4$ for each group). Ribose significantly increased ECM fluorescence. Glucose modified ECM showed increased fluorescence but did not reach statistical significance. Fluorescence intensity was normalized to native ECM. (b) Pepsin extractability was significantly reduced in both glucose and ribose modified ECM compared to native ECM ($n = 4$ for each group), suggesting formation of fluorescent crosslinking (e.g. pentosidine) in ribose modified ECM and non-fluorescent crosslinks in glucose modified ECM. Data is shown as the mean ± SEM. * denotes statistical significance ($p < 0.05$) based on Welch's ANOVA with post-hoc Dunnett's T3 testing.

manually isolated from the kidneys of normal FVB mice using methods similar to those described previously [23,49]. Kidneys were removed from anesthetized mice and sliced into thin transverse sections. Sections were transferred to tubule isolation buffer consisting of (in mM): 130 NaCl, 4 KCl, 2.5 NaH$_2$PO$_4$, 1.2 MgSO$_4$, 6 L-alanine, 0.1 L-arginine, 1.0 trisodium citrate, 5.5 glucose, 2 calcium dilactate, and 10 HEPES, pH 7.4 [50]. Tubules were isolated on a cooled dissecting microscope using fine tipped forceps. Glomeruli were isolated from the kidneys of six-month-old Yorkshire breed pigs. Tissue was acquired from Lampire Biologicals (Pipersville, PA). Glomeruli were isolated by differential sieving using a similar method to that described previously [51]. The renal cortex was dissected, minced and successively passed through 250 and 150 μm sieves (W.S. Tyler, Mentor, OH) and glomeruli were collected on a 32 μm sieve.

Tubular basement membrane stress-strain measurements

To characterize the stress-strain response of tubular basement membrane, we used a custom microcantilever force measurement system that we have previously used to evaluate the mechanical properties of multiple basement membrane systems [23,24]. A detailed description of the technique including microcantilever force-displacement calibration can be found in Bhave et al. [23]. Briefly, isolated tubules were clamped by vacuum applied to a holding pipette and a measurement cantilever with pre-calibrated force-displacement response. The holding pipette was translated a fixed distance to

stretch the tubule while bending the cantilever. The applied force was calculated from the displacement of the pre-calibrated force measurement cantilever. The stretch ratio (λ), was determined from the ratio of the deformed to undeformed length of the tubule. Displacements were determined by automated motion analysis software (WINanalyze). The mathematical model described by Humphrey and Yin [35] was used to describe the stress-strain response of the TBM. This model has been widely employed to evaluate the non-linear mechanical behavior of biological tissue and is described using by Eqs. (1)–(3) based on the functional form described by Martins et al. [36].

$$\sigma = F\frac{\lambda}{A} \qquad (1)$$

$$\sigma = 2\left(\lambda^2 - \frac{1}{\lambda}\right)\left[c_1 c_2 e^{c_2(I_1 - 3)}\right] \qquad (2)$$

$$I_1 = \lambda^2 + \frac{2}{\lambda} \qquad (3)$$

where σ is the stress, F is the applied force, λ is the stretch ratio, A is the cross-sectional area, I_1 is the Right Cauchy-Green tensor, and c_1 and c_2 are the material parameters that were fit to the experimental data by non-linear least-squares analysis in Excel [52]. The cross-sectional area of the TBM was calculated based on previously measured mouse TBM thickness of 193 nm [23]. We and others have

shown the cellular component of the tubule has minimal influence on the resistance of the tubule to tensile or radial deformation [23,53]. As such, measurements of the intact tubules are a measure of the TBM mechanical response.

Glomerular ECM stiffness measurements

To measure glomerular ECM stiffness, we modified the TBM technique to allow for mechanical analysis of glomeruli in compression. In this case a platform was attached to the end of the measurement cantilever and glomeruli were translated into the platform using a micromanipulator to compress the glomerulus and displace the cantilever (Fig. 6). For glomeruli, we found that the cellular component of the glomerulus was a significant contributor to stiffness (data not shown). The contribution of the cellular component of glomeruli to their resistance to compressive deformation is consistent with other techniques used to evaluate glomerular mechanics [42]. In order to determine the properties of the ECM, glomeruli were decellularized by detergent extraction of cells with 1% sodium dodecyl sulfate (SDS) prior to analysis. The compressive modulus of acellular glomeruli were calculated using the mathematical model described by Tatara for compression of a sphere between two flat plates as described by

Eqs. (4)–(7) [54].

$$\delta = \frac{3(1-v^2)F}{4Ea} - \frac{f(a)F}{\pi E} \qquad (4)$$

$$f(a) = \frac{2(1+v)R^2}{\left(a^2 + 4R^2\right)^{3/2}} + \frac{1-v^2}{\left(a^2 + 4R^2\right)^{1/2}} \qquad (5)$$

$$a = (R-\delta)\tan\theta \qquad (6)$$

$$\theta = \cos^{-1}\left(\frac{R-\delta}{R}\right) \qquad (7)$$

where δ is the displacement, F is applied force, E is elastic modulus, a is the radius of contact area between the glomerulus and the cantilever, R is the radius of the non-deformed glomerulus, v is Poisson's ratio which was taken as 0.5, and θ is the angle between the midpoint of the glomerulus and the edge of the contact area. Data were expressed in terms of the degree of compression (δ/R). This model has been shown effective for $\delta/R \leq 0.2$ (up to
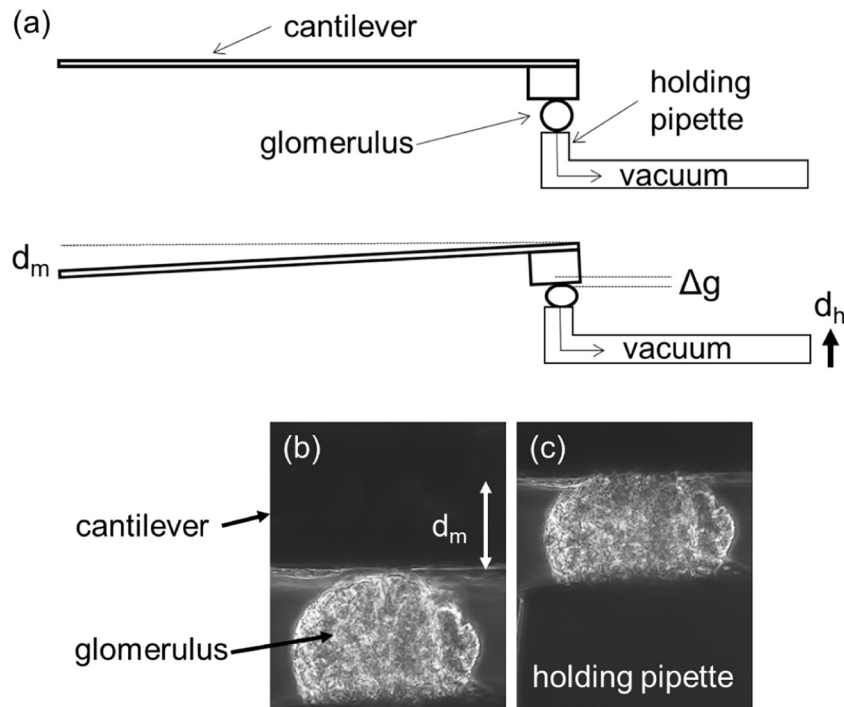
Fig. 6. (a) Schematic of glomerular ECM compression technique. The decellularized glomerulus is held in place with a holding pipette under vacuum. The glomerular ECM is compressed against a force calibrated cantilever. The holding pipette is translated a fixed distance (d_h) and the displacement of the cantilever (d_m) and the compression of the glomerulus (Δg) are used to determine the force/displacement response. (b, c) Imaging of the uncompressed and compressed glomerulus, respectively, showing the cantilever and holding pipette displacements.

20% compression) [55]. Therefore, elastic modulus was determined by fitting E to the experimental data using non-linear least-squares analysis for δ/R from 0 to 0.2. For evaluating the effects of sugar-induced modification on ECM mechanical properties, tubules and glomeruli were incubated in 100 mM glucose or ribose in phosphate buffer for 4 weeks at 37 °C.

Characterization of decellularized glomeruli

To evaluate the structure of the decellularized glomeruli and determine if structural proteins were retained in the matrix following decellularization, glomerular ECM was analyzed by western blotting and immunofluorescence imaging. For western blotting, decellularized matrix was suspended in reducing samples buffer with 8% β-mercaptoethanol. Samples were denatured by heating at 70 °C for 20 min with agitation. Samples were centrifuged at 10,000 ×g for 10 min and supernatants were resolved by SDS-PAGE and transferred to PVDF membranes. Membranes were blocked with 5% milk and were probed with rabbit collagen IV (ab6586 Abcam) or rabbit laminin (ab11575 Abcam) primary antibodies and an HRP-conjugated anti-rabbit secondary antibody. For immunostaining, glomerular matrix was fixed in 4% paraformaldehyde for 20 min on ice followed by three washes in PBS. Decellularized glomeruli were embedded in Histogel at 65 °C for 30 min to aid in tissue sectioning. Histogel embedded decellularized glomeruli were then paraffin embedded and processed by standard histological techniques. Sections were deparaffinized, subjected to antigen retrieval, blocked with BSA, and probed with rat α3 collagen IV (Chondrex 7076) or rabbit laminin antibodies. Sections were washed and probed with FITC anti-rat or Alexa Fluor 555 anti-rabbit secondary antibodies and mounted in mounting media. Nuclei were stained with DAPI in cellularized and decellularized glomeruli. Images were acquired on a standard epifluorescence microscope (Zeiss Axioskop 2).

Biochemical analysis of glycated ECM

As a measure of AGE formation, ECM fluorescence was measured in native and glycated ECM. Fluorescence measurements are commonly used as a measure of AGE formation in tissue, blood, and urine [56,57]. Decellularized porcine cortical ECM, which primarily consists of tubular and glomerular matrix, was incubated in glucose or ribose as described previously. Native and glycated ECM was lyophilized and approximately 5 mg (dry weight) of ECM was hydrolyzed for 20 h in 6 M HCl at 110 °C. Hydrolyzed ECM was concentrated on a Speedvac. Dehydrated samples were dissolved in deionized (DI) water and filtered through a 0.2 μm syringe filter. Fluorescence analysis was performed on a plate reader (Promega Glomax Discover) with an excitation wavelength of 365 nm and an emission of 415–445 nm. The fluorescence signal was normalized to dry mass.

To further evaluate matrix crosslinking, native and glycated ECM samples were subjected to limited pepsin digestion. Samples were homogenized in 0.5 M acetic acid with 1 mg/ml pepsin at a sample to digestion solution ratio of 1:250 weight/volume. Samples were digested for 24 h at 4 °C with constant agitation. Undigested fractions were pelleted by centrifugation. Pepsin digested fractions were concentrated on a Speedvac. Pepsin soluble and insoluble fractions were hydrolyzed and processed as described above. Hydroxyproline concentration was measured using the chloramine T colorimetric assay [58,59]. The ratio of hydroxyproline content in the pepsin digested fraction to the undigested fraction was used as a relative measure of crosslinking. Data were normalized to tissue dry weight.

Data analysis

For data that did not meet the assumption of normality and equal variance, statistical significance was determined using Kruskal-Wallis H testing followed by post-hoc Mann-Whitney U testing for pairwise comparisons. For normally distributed data that did not meet the assumption of equal variance, statistical significance was evaluated by Welch's ANOVA followed by post-hoc Dunnett's T3 testing for multiple comparisons. All analyses were performed in SPSS with statistical significance was set at $p < 0.05$.

Supplementary data to this article can be found online at https://doi.org/10.1016/j.mbplus.2020.100035.

Declaration of competing interest

The authors declare that they have no known competing financial interests or personal relationships that could have appeared to influence the work reported in this paper.

Acknowledgements

References

[1] P.D. Yurchenco, Basement membranes: cell scaffoldings and signaling platforms, Cold Spring Harbor Perspectives in Biology 3 (2011) a004911.

[2] R.T. Miller, Mechanical properties of basement membrane in health and disease, Matrix Biology 57–58 (2017) 366–373.

[3] D.E. Discher, P. Janmey, Y.-l. Wang, Tissue cells feel and respond to the stiffness of their substrate, Science 310 (2005) 1139–1143.

[4] R.G. Wells, The role of matrix stiffness in regulating cell behavior, Hepatology 47 (2008) 1394–1400.

[5] W. Ramos-Lewis, A. Page-McCaw, Basement membrane mechanics shape development: lessons from the fly, Matrix Biology 75–76 (2019) 72–81.

[6] T.R. Cox, J.T. Erler, Remodeling and homeostasis of the extracellular matrix: implications for fibrotic diseases and cancer, Disease Models & Mechanisms 4 (2011) 165–178.

[7] P. Lu, V.M. Weaver, Z. Werb, The extracellular matrix: a dynamic niche in cancer progression, The Journal of Cell Biology 196 (2012) 395–406.

[8] F. Bordeleau, B.N. Mason, E.M. Lollis, M. Mazzola, M.R. Zanotelli, S. Somasegar, J.P. Califano, C. Montague, D.J. LaValley, J. Huynh, N. Mencia-Trinchant, Y.L.N. Abril, D.C. Hassane, L.J. Bonassar, J.T. Butcher, R.S. Weiss, C.A. Reinhart-King, Matrix stiffening promotes a tumor vascular phenotype, Proceedings of the National Academy of Sciences of the United States of America 114 (2017) 492–497.

[9] A.C. Brown, V.F. Fiore, T.A. Sulchek, T.H. Barker, Physical and chemical microenvironmental cues orthogonally control the degree and duration of fibrosis-associated epithelial-to-mesenchymal transitions, The Journal of Pathology 229 (2013) 25–35.

[10] J.C. Hewlett, J.A. Kropski, T.S. Blackwell, Idiopathic pulmonary fibrosis: epithelial-mesenchymal interactions and emerging therapeutic targets, Matrix Biology 71–72 (2018) 112–127.

[11] P. Pakshir, B. Hinz, The big five in fibrosis: macrophages, myofibroblasts, matrix, mechanics, and miscommunication, Matrix Biology 68–69 (2018) 81–93.

[12] A.-M. Baker, D. Bird, G. Lang, T.R. Cox, J.T. Erler, Lysyl oxidase enzymatic function increases stiffness to drive colorectal cancer progression through FAK, Oncogene 32 (2013) 1863–1868.

[13] K.R. Leventhal, H. Yu, L. Kass, J.N. Lakins, M. Egeblad, J.T. Erler, S.F.T. Fong, K. Csiszar, A. Giaccia, W. Weninger, M. Yamauchi, D.L. Gasser, V.M. Weaver, Matrix crosslinking forces tumor progression by enhancing integrin signaling, Cell 139 (2009) 891–906.

[14] J.M. Forbes, M.E. Copper, M.D. Oldfield, M.C. Thomas, Role of advanced glycation end products in diabetic nephropathy, Journal of the American Society of Nephrology 14 (2003) S254–S258.

[15] D.R. Sell, K.M. Biemel, O. Reihl, M.O. Lederer, C.M. Strauch, V.M. Monnier, Glucosepane is a major protein cross-link of the senescent human extracellular matrix: relationship with diabetes, The Journal of Biological Chemistry 280 (2005) 12310–12315.

[16] D.R. Sell, E.C. Carlson, V.M. Monnier, Differential effects of type 2 (non-insulin-dependent) diabetes mellitus on pentosidine formation in skin and glomerular basement membrane, Diabetologia 36 (1993) 936–941.

[17] N. Verzijl, J. DeGroot, C.B. Zaken, O. Braun-Benjamin, A. Maroudas, R.A. Bank, J. Mizrahi, C.G. Schalkwijk, S.R. Thrope, J.W. Baynes, J.W.J. Bijlsma, F.P.J.G. Lafeber, J.M. TeKoppele, Crosslinking by advanced glycation end products increases the stiffness of the collagen network in human articular cartilage, Arthritis and Rheumatism 46 (2002) 114–123.

[18] D. Vashishth, G.J. Gibson, J.I. Khoury, M.B. Schaffler, J. Kimura, D.P. Fyhrie, Influence of nonenzymatic glycation on biomechanical properties of cortical bone, Bone 28 (2001) 195–201.

[19] G.K. Reddy, Cross-linking in collagen by nonenzymatic glycation increases the matrix stiffness in rabbit achilles tendon, Experimental Diabesity Research 5 (2004) 143–153.

[20] J.H. Miner, Glomerular basement membrane composition and the filtration barrier, Pediatric Nephrology 26 (2011) 1413–1417.

[21] D.R. Abrahamson, V. Leardkamolkarn, Development of kidney tubular basement membranes, Kidney International 39 (1991) 382–393.

[22] R. Lennon, A. Byron, J.D. Humphries, M.J. Randles, A. Carisey, S. Murphy, D. Knight, P.E. Brenchley, R. Zent, M.J. Humphries, Global analysis reveals the complexity of the human glomerular extracellular matrix, J. Am. Soc. Nephrol. 25 (2014) 939–951.

[23] G. Bhave, S. Colon, N. Ferrell, The sulfilimine cross-link of collagen IV contributes to kidney tubular basement membrane stiffness, American Journal of Physiology. Renal Physiology 313 (2017) F596–F602.

[24] A.M. Howard, K.S. LaFever, A.M. Fenix, C.R. Scurrah, K.S. Lau, D.T. Burnette, G. Bhave, N. Ferrell, A. Page-McCaw, DSS-induced damage to basement membranes is repaired by matrix replacement and crosslinking, Journal of Cell Science 132 (2019)(jcs226860).

[25] C. Storm, J.J. Pastore, F.C. MacKintosh, T.C. Lubensky, P.A. Janmey, Nonlinear elasticity in biological gels, Nature 435 (2005) 191–194.

[26] S. Motte, L.J. Kaufman, Strain stiffening in collagen I networks, Biopolymers 99 (2013) 35–46.

[27] M.L. Gardel, J.H. Shin, F.C. MacKintosh, L. Mahadevan, P. Matsudaira, D.A. Weitz, Elastic behavior of cross-linked and bundled actin networks, Science 304 (2004) 1301–1305.

[28] J. Zhou, Y.C. Fung, The degree of nonlinearlity and anisotropy of blood vessel elasticity, Proceedings of the National Academy of Sciences of the United States of America 94 (1997) 14255–14260.

[29] R.J. Petrie, N. Gavara, R.S. Chadwick, K.M. Yamada, Nonpolarized signaling reveals two distinct modes of 3D cell migration, The Journal of Cell Biology 197 (2012) 439–455.

[30] R.K. Das, V. Gocheva, R. Hammink, O.F. Zouani, A.E. Rowan, Stress-stiffening-mediated stem-cell commitment switch in soft responsive hydrogels, Nature Materials 15 (2016) 318–325.

[31] O. Chaudhuri, L. Gu, M. Darnell, D. Klumpers, S.A. Bencherif, J.C. Weaver, N. Huebsch, D.J. Mooney, Substrate stress relaxation regulates cell spreading, Nature Communications 6 (2015) 6364.

[32] J.P. Winer, S. Oake, P.A. Janmey, Non-linear elasticity of extracellular matrices enables contractile cells to communicate local position and orientation, PLoS One 4 (2009) (e6382).

[33] M. Jaspers, M. Dennison, M.F.J. Mabesoone, F.C. MacKintosh, A.E. Rowan, P.H.J. Kouwer, Ultra-responsive soft matter from strain-stiffening hydrogels, Nature Communications 5 (2014) 5808.

[34] M. Jaspers, S.L. Vaessen, P. von Schayik, D. Voerman, A. E. Rowan, P.H.J. Kouwer, Nonlinear mechanics of hydrid polymer networks that mimic the complex mechanical environment of cells, Nature Communications 8 (2017) 15487.

[35] J.D. Humphrey, F.C.P. Yin, On constitutive relations and finite deformations of passive cardiac tissue: I. A pseudo-strain-energy function, Journal of Biomedical Engineering 109 (1987) 298–304.

[36] P.A.L.S. Martins, R.M.N. Jorge, A.J.M. Ferreira, A comparative study of several material models for prediction of hyperelastic properties: application to silicone-rubber and soft tissues, Strain 42 (2006) 135–147.

[37] F. Safshekan, M. Tafazzoli-Shadpour, M. Abdouss, M.B. Shadmehr, Mechanical characterization and constitutive modeling of human trachea: age and gender dependency, Materials 9 (2016) 456.

[38] D. Laroque, C. Inisan, C. Berger, E. Vouland, L. Dufosse, F. Guerard, Kinetic study on the Maillard reaction. Consideration of sugar reactivity, Food Chemistry 111 (2008) 1032–1042.

[39] R.G. Khalifah, P. Todd, A.A. Booth, S.X. Yang, J.D. Mott, B.G. Hudson, Kinetics of nonenzymatic glycation of ribonuclease A leading to advanced glycation end products. Paradoxical inhibition of ribose leads to facile isolation of protein intermediates for rapid post-Amadori studies, Biochemistry 35 (1996) 4645–4654.

[40] D.R. Sell, V.M. Monnier, Structure elucidation of a senescence cross-link from human extracellular matrix, The Journal of Biological Chemistry 264 (1989) 21597–21602.

[41] G.E. Sroga, A. Siddula, D. Vashishth, Glycation of human cortical and cancellous bone captures differences in the formation of Maillard reaction products between glucose and ribose, PLoS One 10 (2015)e0117240.

[42] A.E. Embry, H. Mohammadi, X. Niu, L. Liu, B. Moe, W.A. Miller-Little, C.Y. Lu, L.A. Bruggeman, C.A. McCulloch, P. A. Janmey, R.T. Miller, Biochemical and cellular determinants of renal glomerular elasticity, PLoS One 11 (2016) e167924.

[43] A.R. Harris, L. Peter, J. Bellis, B. Baum, A.J. Kabla, G.T. Charras, Characterizing the mechanics of cultured cell monolayers, Proceedings of the National Academy of Sciences of the United States of America 109 (2012) 16449–16454.

[44] A.R. Harris, G.T. Charras, Experimental validation of atomic force microscopy-based cell elasticity measurements, Nanotechnology 22 (2011) 345102.

[45] P.A. Voziyan, R.G. Khalifah, C. Thibaudeau, A. Yildiz, J. Jacob, A.S. Serianni, B.G. Hudson, Modification of proteins _in vitro_ by physiological levels of glucose, The Journal of Biological Chemistry 278 (2003) 46616–46624.

[46] R. Ramasamy, S.J. Vannucci, S.S.D. Yan, K. Herold, S.F. Yan, A.M. Schmidt, Advanced glycation end products and RAGE: a common thread in aging, diabetes, neurodegeneration, and inflammation, Glycobiology 15 (2005) 16R–28R.

[47] R. Ramasamy, S.F. Yan, A.M. Schmidt, Receptor for AGE (RAGE): signaling mechanisms in the pathogenesis of diabetes and its complications, Annals of the New York Academy of Sciences 1243 (2011) 88–102.

[48] J.D. Mott, R.G. Khalifah, H. Nagase, C.F Shield III, J.K. Hudson, B.G. Hudson, Nonenyzmatic glycation of type IV collagen and matrix metalloproteinase susceptibility, Kidney International 52 (1997) 1302–1312.

[49] P.D. Cabral, N.J. Hong, A.H. Khan, P.A. Ortiz, W.H. Beierwaltes, J.D. Imig, J.L. Garvin, Fructose stimulates Na/H exchange activity and sensitizes the proximal tubule to angiotensin II, Hypertension 63 (2014) e68–e73.

[50] P.D. Cabral, N.J. Hong, J.L. Garvin, Shear stress increases nitric oxide production in thick ascending limbs, American Journal of Physiology. Renal Physiology 299 (2010) F1185–F1192.

[51] J.I. Kreisberg, R.L. Hoover, M.J. Karnovsky, Isolation and characterization of rat glomerular epithelial cells in vitro, Kidney International 14 (1978) 21–30.

[52] D.C. Harris, Nonlinear least-squares curve fitting with Microsoft Excel solver, Journal of Chemical Education 75 (1998) 119–121.

[53] L.W. Welling, J.J. Grantham, Physical properties of isolated perfused renal tubules and tubular basement membranes, The Journal of Clinical Investigation 51 (1972) 1063–1075.

[54] Y. Tatara, Large deformations of a rubber sphere under diametral compression part 1: theoretical analysis of press approach, contact radius and lateral extension, JSME International Journal. Ser. A, Mechanics and Material Engineering 36 (1993) 190–196.

[55] K. Kim, J. Cheng, Q. Liu, X.Y. Wu, Y. Sun, Investigation of mechanical properties of soft hydrogel microcapsules in relation to protein delivery using a MEMS force sensor, Journal of Biomedical Materials Research. Part A 92 (2010) 103–113.

[56] T. Soulis-Liparota, M. Cooper, D. Papazoglou, B. Clarke, G. Jerums, Retardation by aminoguanidine of development of albuminuria, mesangial expansion, and tissue fluorescence in streptozocin-induced diabetic rat, Diabetes 40 (1991) 1328–1334.

[57] K. Yanagisawa, Z. Makita, K. Shiroshita, T. Ueda, T. Fusegawa, S. Kuwajima, M. Takeuchi, T. Koike, Specific fluorescence assay for advanced glycation end products in blood and urine of diabetic patients, Metabolism 47 (1998) 1348–1353.

[58] D.D. Cissell, J.M. Link, J.C. Hu, K.A. Athanasiou, A modified hydroxyproline assay based on hydrochloric acid in Ehrlich's solution accurately measures tissue collagen content, Tissue Engineering. Part C, Methods 23 (2017) 243–250.

[59] C.A. Edwards, W.D. O'Brien Jr., Modified assay for determination of hydroxyproline in a tissue hydrolysate, Clinica Chimica Acta 104 (1980) 161–167.